American Journal of Pathology, Vol. 166, No. 6, June 2005

Tumorigenesis and Neoplastic Progression

Identification of Novel Candidate Oncogenes and Tumor Suppressors in Malignant Pleural Mesothelioma Using Large-Scale Transcriptional Profiling

Gavin J. Gordon,* Graham N. Rockwell,† Roderick V. Jensen,‡ James G. Rheinwald,§ Jonathan N. Glickman,¶ Joshua P. Aronson,* Brian J. Pottorf,* Matthew D. Nitz,* William G. Richards,* David J. Sugarbaker,* and Raphael Bueno*

From the Thoracic Surgery Oncology Laboratory, the Division of Thoracic Surgery, and the Departments of Neurology,† Dermatology,§ and Pathology,¶ Brigham and Women's Hospital, Harvard Medical School, Boston, Massachusetts; and the Department of Physics,‡ University of Massachusetts, Boston, Massachusetts*

Malignant pleural mesothelioma (MPM) is a highly lethal, poorly understood neoplasm that is typically associated with asbestos exposure. We performed transcriptional profiling using high-density oligonucleotide microarrays containing ~22,000 genes to elucidate potential molecular and pathobiological pathways in MPM using discarded human MPM tumor specimens ($n = 40$), normal lung specimens ($n = 4$), normal pleura specimens ($n = 5$), and MPM and SV40-immortalized mesothelial cell lines ($n = 5$). In global expression analysis using unsupervised clustering techniques, we found two potential subclasses of mesothelioma that correlated loosely with tumor histology. We also identified sets of genes with expression levels that distinguish between multiple tumor subclasses, normal and tumor tissues, and tumors with different morphologies. Microarray gene expression data were confirmed using quantitative reverse transcriptase-polymerase chain reaction and protein analysis for three novel candidate oncogenes (*NME2*, *CRI1*, and *PDGFC*) and one candidate tumor suppressor (*GSN*). Finally, we used bioinformatics tools (ie, software) to create and explore complex physiological pathways. Combined, all of these data may advance our understanding of mesothelioma tumorigenesis, pathobiology, or both. *(Am J Pathol 2005, 166:1827–1840)*

Malignant pleural mesothelioma (MPM) is a highly lethal malignancy primarily resulting from previous asbestos exposure.[1,2] Approximately 3000 patients are diagnosed with MPM in the US annually and the incidence worldwide is projected to rise substantially in the next 2 decades.[3–5] Treatment options are few and most patients die within 2 years of diagnosis. The pathological diagnosis of MPM is often complex and requires immunohistochemical staining with a panel of antibodies. There are three distinct histological subtypes of MPM based on the microscopic appearance of the major malignant elements: epithelial, sarcomatoid, mixed. The majority of MPMs are epithelial (50%). Patients with this subtype are generally thought to experience a somewhat longer survival than do patients with the other subtypes.[6,7] However, clinicians have long noticed a certain degree of variability in patient survival and response to therapy that is not explained solely by the stage or histological appearance and may therefore be due to more subtle biological variability among tumors.

The long latency period between asbestos exposure and tumor development implies that multiple, and likely diverse, genetic changes are required for the malignant transformation of mesothelial cells. Several oncogenes and tumor suppressors have been hypothesized to play a

Supported in part by the Brigham Surgical Group Foundation (to G.J.G.), the Cancer Research and Prevention Foundation (to G.J.G.), the National Cancer Institute (CA-105249-02 to G.J.G. and CA-102591-01 and CA-100315-01 to R.B.), the Mesothelioma Applied Research Foundation (to G.J.G. and R.B.), and the Vancouver Foundation (to R.B.).

Accepted for publication March 2, 2005.

Supplemental material can be found on http://ajp.amjpathol.org.

Address reprint requests to Gavin J. Gordon, Ph.D., or Raphael Bueno, M.D., Brigham and Women's Hospital, Division of Thoracic Surgery, 75 Francis St., Boston, MA 02115. E-mail: ggordon@partners.org or rbueno@partners.org.

role in MPM carcinogenesis.[8] These include the tumor suppressors *RASSF1A*, *NF2*, and *p16* as well as the growth factors/proto-oncogenes/signaling molecules c-*fos*, c-*jun*, *EGF*, *VEGF*, *MetAP2*, c-*Met*, c-*myc*, and *fra-1*. Of note, MPM does not appear to involve aberrant expression of many well-studied growth control genes such as *H-ras*, *K-ras*, *p53*, and *Rb*[9–11] although SV40 T antigen has been proposed to inactivate *p53* function in some MPM tumors.[12]

Large-scale transcriptional studies using microarrays have been reported in multiple cancers. To date, studies of this sort reported for MPM have used relatively small numbers of tissues and/or cell lines.[13–16] This is likely the consequence of the relatively low incidence of MPM and by extension, the difficulty of acquiring large numbers of MPM pathological specimens. One exception is a recent study by Pass and colleagues.[17] These investigators profiled 21 MPM patients and created a 27-gene neural network classifier that could predict clinical outcome with moderate accuracy. Previously, we profiled 31 MPM tumors to develop and validate a six-gene diagnostic test for MPM[13] and a four-gene prognostic test for patients undergoing cytoreductive surgery.[18] In the current study, we profile 40 MPM tumors, as well as normal lung and pleural tissues ($n = 9$), and tumor-derived and nontumorigenic cell lines ($n = 5$) using microarrays containing ~22,000 genes to validate a previously described MPM diagnostic test[13] and better characterize the molecular pathways involved in the pathogenesis of MPM.

Materials and Methods

Tissues and Cell Lines Profiled Using Microarrays

Discarded MPM surgical specimens ($n = 40$), normal pleura specimens ($n = 5$), and normal lung specimens ($n = 4$) were freshly collected (and snap-frozen) from patients who underwent surgery at Boston's Brigham and Women's Hospital (BWH) between October 1998 and August 2000. All of these patients underwent extrapleural pneumonectomy with heated intrapleural *cis*-platin chemotherapy delivered after the specimens were removed. All normal specimens were obtained from patients who were never diagnosed with MPM. Two human MPM cell lines (MS589 and MS428) were kindly provided by Jonathan A. Fletcher, M.D., Department of Pathology, BWH. The JMN1B MPM cell line[19,20] has been described previously. The SV40-immortalized, nontumorigenic mesothelial cell line (Met-5A)[21] and the MPM cell line MSTO-211H[22] were purchased from the American Type Culture Collection (Rockville, MD). Normal tissues were obtained from additional consented patients undergoing treatment for diseases other than MPM. All MPM samples used in these studies contained relatively pure tumor (greater than 50% tumor cells per high-power field examined in a section adjacent to the tissue used). The microscopic slides from the patients' resection specimens were reviewed by one of the authors (J.G.), and the diagnosis and histological subclassification of MPM confirmed in all cases. Linked clinical and pathological data were obtained for all patients who contributed tumor specimens. Specimens and data were rendered anonymous to protect patient confidentiality. Studies using human tissues were approved by and conducted in accordance with the policies of the Institutional Review Board at BWH.

Microarray Experiments

For preparation of RNA for microarray analysis, JMN1B, MS589, MS428, MSTO-211H, and Met5A cells were grown in RPMI 1640 medium (Invitrogen Life Technologies, Carlsbad, CA) supplemented with 10% calf serum. Sample preparation and hybridization to Affymetrix human U133A oligonucleotide probe arrays was performed essentially as described in the Affymetrix Expression Analysis Technical Manual using total RNA (7 μg) that was prepared from whole tumor blocks and cells in exponential growth using TRIzol reagent (Invitrogen Life Technologies). Hybridization experiments were scanned visually for artifacts and gene expression levels (ie, Affymetrix signal) for each microarray were generated and scaled to a target intensity of 100 using Affymetrix Microarray Suite v.5.0 (Sants Clara, CA).

Gene Selection and Clustering Algorithms

Before unsupervised cluster analysis and principal components analysis,[23] the expression level of each of the 22,000 genes on the microarray was stated relative to the median value of that gene in all normal samples, tumor samples, and cell lines analyzed and then $\log_2$-transformed. The 1405 most variable transcripts (SD, more than threefold) were chosen to perform cluster analysis using CLUSTER and TREEVIEW software[24] after median centering and normalization of the data. Other clustering algorithms including partitioning around medoids[25] and principal components analysis used the S-PLUS statistical package.[26] Partitioning around medoids is similar to *k*-means clustering, but uses medoids instead of centroids and minimizes a sum of dissimilarities instead of a sum of squared Euclidean distances.

Using S-PLUS, we identified potential tumor molecular markers by determining which of the genes on the microarray was expressed at significantly ($P < 0.05$) different average expression levels between all 40 tumor samples and all (lung and pleura) normal samples using a two-sided Student's (parametric) *t*-test for pair-wise comparisons of average gene expression levels. Genes discriminatory between subclasses discovered during cluster analysis and between epithelial and mixed MPM histological subtypes were similarly identified. The SAM algorithm[27] was used to estimate the false discovery rate.

Pathway Analysis of Candidate MPM Oncogenes

Pathway analysis was performed using Ingenuity pathways analysis (*www.ingenuity.com*), a web-delivered ap-

plication that enables biologists to discover, visualize, and explore potentially relevant pathobiological networks. Genes found to be statistically significantly upregulated in MPM so identified were used to create a total of 12 pathway networks. Seven of these networks with at least one gene in common were subsequently merged for display. The combined network is displayed graphically as nodes (genes/gene products) and edges (the biological relationships between the nodes). The length of an edge reflects the evidence supporting that node-to-node relationship. Edges supported by more articles from the literature are shorter. For simplicity, genes are referred to by their LocusLink symbol.

Quantitative Reverse Transcriptase (RT)-Polymerase Chain Reaction (PCR)

For preparation of RNA for quantitative RT-PCR analysis, MS589, MS428, MS924, JMN1B, and the normal primary human mesothelial cell line HM3[28,29] were grown in M199/MCDB105 [1:1 (v/v) medium + 15% newborn calf serum + 0.4 μg/ml hydrocortisone] with or without epidermal growth factor (EGF) (10 ng/ml). This medium is permissive for growth both of normal and neoplastic human mesothelial cells.[28,29] Note that HM3 cells and MS924 cells were used only for quantitative RT-PCR analysis and were not analyzed using microarrays. MS924 was kindly provided by Jonathan A. Fletcher, M.D., Department of Pathology, BWH. All cells were maintained in a humidified 5% CO_2 incubator at 37°C.

Quantitative RT-PCR was performed using a SYBR-Green fluorometric-based detection system and reagents purchased from Applied Biosystems (Foster City, CA; *www.appliedbiosystems.com*, see technical bulletin no. 4310251 for details and protocol). Using TRIzol reagent, we isolated total RNA (2 μg) from frozen tumor specimens, preconfluent, exponentially growing cultures, or mitogen-deprived growth-arrested cultures. The isolated RNA was then reverse-transcribed into complementary DNA (cDNA) with the use of *Taq*-Man reverse transcription reagents (Applied Biosystems), and quantified using all controls recommended by the manufacturer. Both culture conditions (ie, ±EGF) permit the growth of the mesothelioma lines but the −EGF condition induces a growth-arrested state for HM3 cells, as described previously.[28] All RT-PCR primers were used at a final concentration of 800 nmol/L in the reaction mixture. (For simplicity, genes are referred to by their LocusLink symbol.) Primer sequences have been previously published for *GAPD*,[30] *CALB2* (calretinin),[13] *CLDN7* (claudin-7),[13] ANXA8 (annexin A8, also known as vascular anticoagulant-β, VAC-β),[13] *TACSTD1* (tumor-associated calcium signal transducer 1),[13] *CD200* (also known as MRC OX-2),[13] *TITF1* (thyroid transcription factor 1).[13] Other primers (synthesized by Invitrogen Life Technologies) were as follows (forward and reverse): *NME2* (5′-GACCTGAAAGACCGACCATT-3′ and 5′-AATCTGCTGGATTGGTCTCC-3′), *PDGFC* (5′-TGTCATGCCACAATTCACAG-3′ and 5′-TGCCATCTCTCTGGTTCAAG-3′), *CRI1* (5′-TGCCGGCTACAGAGTATCAG-3′ and 5′-ACTGATCAAACGGGGT-CTTC-3′), *GSN* (5′-ACGGCTGAAGGACAAGAAGA-3′ and 5′-TTCCAACCCAGACAAAGACC-3′). PCR amplification of cDNA was performed using a Stratagene MX 3000P device with appropriate controls. The comparative CT equation (Applied Biosystems) describes the exponential nature of PCR-based amplification and was used exactly as stated to measure the relative expression levels of *NME2*, *PDGFC*, and *CRI1* relative to those of *GAPDH*.

Western Blot Analysis

To prepare the cell lysates for Western blot analysis, 98-483, H-2052, JMN1B, MS589, MS428, MSTO-211H, and Met5A cells were grown in RPMI 1640 medium (Invitrogen Life Technologies) supplemented with 10% calf serum. Note that 98-483 and H-2052 cells were used only in Western blot analysis and were not analyzed using microarrays or quantitative RT-PCR. The 98-483 MPM cell line was kindly provided by Jonathan A. Fletcher, M.D. The H-2052 MPM cell line was purchased from American Type Culture Collection. Cell lines subjected to protein analysis were homogenized and lysed at 4°C in a buffer containing 20 mmol/L Tris-HCl (pH = 8), 137 mmol/L NaCl, 2 mmol/L ethylenediamine tetraacetic acid, 10% glycerol, 1% Nonidet P-40, 200 mmol/L sodium orthovanadate, 1 mmol/L dithiothreitol, 1 mmol/L phenylmethyl sulfonyl fluoride, 2 mg/ml leupeptin, and 5 mg/ml aprotinin. The normal pleura protein preparation was similarly made by pooling the five normal pleura specimens analyzed using microarrays. Protein quantity was estimated using the Bio-Rad protein assay (Bio-Rad, Richmond, CA). For Western blot analysis, aliquots of cell lysates were combined with a protein solubilization stock buffer consisting of 250 mmol/L Tris-HCl (pH 7.4), 2% sodium dodecyl sulfate, 30% glycerol, and 0.01% bromophenol blue (pH 6.8) to a final concentration of 2 μg of protein/μl and denatured by boiling for 5 minutes. Samples containing ~50 μg of protein per lane were separated using sodium dodecyl sulfate-polyacrylamide gel electrophoresis (12% gel) and transferred onto Hybond ECL nitrocellulose membranes (Amersham, Arlington Heights, IL) according to standard procedures. All subsequent incubations were performed at room temperature unless otherwise stated. Nitrocellulose membranes were incubated with agitation overnight at 4°C in a blocking buffer consisting of 5% nonfat dry milk in phosphate-buffered saline (PBS) (136 mmol/L NaCl, 2.7 mmol/L KCl, 10 mmol/L Na_2PO_4, and 1.76 mmol/L KH_2PO_4, pH 7.2) and 0.05% Tween-20. Antibodies specific to human NME2 (Santa Cruz Biotechnology, Santa Cruz, CA), GSN (Research Diagnostics, Flanders, NJ), CRI1 (AKA EID-1, U.S. Biological, Swampscott, MA), and β-actin (Sigma, St. Louis, MO) were diluted 1:100 in PBS (for NME2), used at 2 μg/ml in PBS (for CRI1), diluted 1:3000 in PBS (for GSN), and diluted 1:500 in PBS (for β-actin) for 1 hour of incubation at room temperature. Horseradish peroxidase-conjugated secondary antibodies (DAKO,

Carpinteria, CA) were diluted 1:10,000 in PBS. Membranes were washed after the primary and secondary antibodies in three changes of 0.05% Tween 20 in PBS for 5 minutes each. Chemiluminescent detection was performed using ECL reagents (Amersham) and the size of protein bands estimated by comparison to Full Range Rainbow molecular marker standard (Amersham).

Immunohistochemistry

Indirect immunoperoxidase analysis of NME2 and CRI1 protein was performed on a tissue array consisting of 66 MPM tumors, 2 lung adenocarcinoma tumors, and 4 normal pleura tissues. This array was constructed from the same 40 MPM tumors analyzed using microarrays and an additional 26 formalin-fixed paraffin-embedded MPM tumor tissues obtained from pathological specimens of patients undergoing extrapleural pneumonectomy at BWH. Because the tumors were anonymized after deidentified clinical information was provided, we were not able to directly compare mRNA data from microarrays with protein data from tissue microarrays on a patient-by-patient basis. The microscopic slides from the patients' resection specimens were reviewed by one of the authors (J.G.), and the diagnosis and histological subclassification of MPM confirmed in all cases. Two to four representative 1-mm cores were used for each tumor. Construction of the array was performed by the Dana Farber/Harvard Cancer Center Tissue Microarray Core Facility, and was approved by the BWH Institutional Review Board. For immunostaining, 6-μm sections were cleared with xylenes and rehydrated through a graded series of alcohols. NME2 and CRI1 detection was performed using an accelerated avidin/biotin peroxidase procedure per the manufacturer's recommended protocol (Vectastain ABC Elite kit; Vector Laboratories, Burlingame, CA) and primary antibody concentrations and incubation times identical to those used in Western blot analysis. Endogenous peroxidase activity was quenched by incubation in a 0.3% solution of H_2O_2 in methanol for 5 minutes. Blocking of nonspecific activity was accomplished using diluted serum of the secondary antibody species (Vector Laboratories). Primary antibodies were replaced with PBS as a negative control. Sections were developed in diaminobenzidine (DAB kit, Vector Laboratories), lightly counterstained with Gill's hematoxylin, dehydrated through a graded series of alcohols, and permanently mounted. Images were digitally captured using an Olympus T041 microscope. To quantify protein expression levels, slides were read by a pathologist (J.G.) who was blinded to the gene expression data. Individual tissues were scored as follows: no expression, <25% positive cells, 25 to 50% positive cells, 50 to 75% positive cells, >75% positive cells. The intensity of staining was subjectively scored either as strong or weak. The statistical significance of observed differences was assessed using χ^2 analysis with $P < 0.05$.

Results and Discussion

Unsupervised Cluster Analysis

We have previously profiled 31 MPM tumors using microarrays containing ~12,000 genes and used these data to design a diagnostic test to distinguish MPM from adenocarcinoma of the lung.[13] In the current study, we examined global gene expression profiles of 40 MPM tumors, 9 normal tissues (lung and pleura), and five cell lines using microarrays containing ~22,000 genes. Unlike our initial effort,[13] both of these normal tissue types were included as controls because MPM arises from mesothelial cells of the pleura and frequently envelopes lung tissues. Of the five cell lines, four are MPM-derived and 1 (Met-5A) is a nontumorigenic immortalized mesothelial cell line. For simplicity, genes are referred to by their LocusLink symbol. We did not use samples previously profiled[13] in cluster analysis in the current study because it would substantially limit the number of genes available for use due to inherent platform differences.

Of the 22,000 genes represented on the microarray, we chose 1405 genes with the most variable expression levels across all samples to perform two-dimensional unsupervised cluster analysis. The dendrogram specifying the arrangement of samples is shown in Figure 1 with linked clinical data available in Supplemental Table 1 at *http://ajp.amjpathol.org*. Four distinct subclasses can be seen, two of which consist entirely of MPM samples. These were arbitrarily designated C1 and C2 ($n = 17$ and $n = 14$, respectively; Figure 1). The other two subclasses consist primarily of normal tissues and cell lines (normal and cell, respectively; Figure 1). C1 and C2 tumors consisted almost entirely of epithelial (88%) and mixed (78%) histological subtypes, respectively, demonstrating that varied morphological appearance may have a basis in distinct gene expression patterns. It has been reported using large sample cohorts that patients with epithelial histology generally experience a significantly longer disease-free survival than patients with nonepithelial histology.[5] Nevertheless, we did not find any statistically significant survival differences between C1 and C2 subclasses, possibly because of the relatively small number of specimens examined.

Unexpectedly, a total of nine tumors were not contained within either C1 or C2, and seven of these samples clustered opposite the normal samples. The cause of this observation was not immediately clear, because all MPM samples contained relatively pure tumor content and the seven samples clustering nearest the normal tissues were >90% tumor. Nor did we observe any noticeable or statistically significant trends in clinical data for these nine samples. Although these nine samples were not tightly clustered on a single branch of the dendrogram, we initially hypothesized that these samples represented a third tumor subclass distinct from C1/C2 tumors.

To test this hypothesis, we first used the expression data for the 1405 highly variable genes from above in other unsupervised hierarchical clustering algorithms and found that the general arrangement of samples was maintained. When we excluded normal tissues and cell

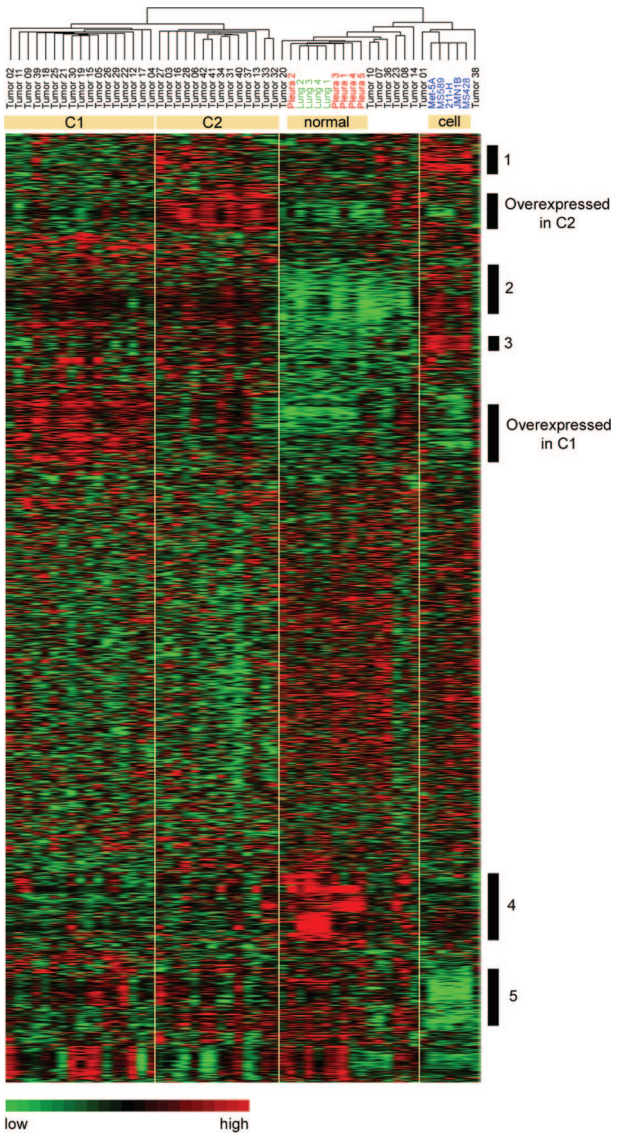

Figure 1. Defining MPM subclasses using unsupervised hierarchical clustering. Two-dimensional unsupervised hierarchical clustering was performed using the 1405 most variable transcripts across MPM tumor samples (n = 40, **black letters**), normal lung samples (n = 4, **green letters**), normal pleura samples (n = 5, **red letters**), and cell lines (n = 5, **blue letters**). The dendrogram specifying the arrangement of samples is shown across the **top** with major nontumor tissue types (ie, normal or cell line) and both major tumor subclasses (ie, C1 and C2) identified using **yellow bars** found immediately below. Individual gene expression levels (in rows) for each sample (in columns) were normalized and expressed relative to the median value for each gene in all samples according to the scale at the **bottom left**. **Bars** to the **right** of the figure refer to regions of differentially expressed genes shown in greater detail in Figures 2 and 3 (for genes overexpressed in subclasses C1 and C2, respectively) and Supplemental Figures 2 to 6 at *http://ajp.amjpathol.org* (for numbered bars 1 to 5, respectively).

lines and repeated the analysis, we found that the resulting dendrogram contained three major subbranches: one contained all C1 tumors, another contained all C2 tumors, and the third contained four of the nine non-C1/C2 samples (tumors 07, 10, 36, and 20), with the remaining five distributed between the C1 subbranch (n = 3) and C2 subbranch (n = 2).

Next we clustered all of the samples using a nonhierarchical algorithm (ie, partitioning around medoids) and the same 1405 genes with six predicted clusters: normal lung, normal pleura, cell lines, C1, C2, and a putative C3 tumor cluster consisting of the nine non-C1/C2 samples from Figure 1. We found that the normal pleura samples, normal lung samples, and cell lines were all assigned to unique clusters in this analysis. Of the three remaining clusters, one contained only C1 tumors, another contained all C2 tumors and four of the nine non-C1/C2 tumors, and the third consisted of five C1 tumors and five of the nine non-C1/C2 tumors

Finally, a three-dimensional graphical display of the results of principal components analysis demonstrates that C1/C2 tumors can be separated easily from normal tissues and the cell lines along the first principal component, while the same cannot be said of the other nine samples (Supplemental Figure 1 at *http://ajp.amjpathol.org*). These combined results suggest that the nine non-C1/C2 samples do not represent a distinct third subclass of MPM. They do not cluster tightly with the majority of MPM tumors in hierarchical cluster analysis likely because they have distinct gene expression patterns at least with respect to a subset of the 1405 genes used in these analyses. The existence of two distinct tumor classes and the nine that do not always cluster within C1 or C2 is consistent with the great biological variability observed *in vivo* as manifested in patient clinical behavior and the diverse cytogenetic features of MPM tumors. This may reflect multiple nonoverlapping carcinogenic pathways in MPM especially considering its extraordinary long latency period.

Genes Distinctive of MPM Subclasses

We observed several groups of genes with distinct expression patterns among cell lines and normal and tumor tissues (Figure 1). Genes highly expressed in subclasses C1 and C2 are listed individually and shown in greater detail in Figures 2 and 3, respectively. Other distinctive gene clusters (delineated by bars 1 to 5 in Figure 1) are listed individually and shown in greater detail in Supplemental Figures 2 through 6 at *http://ajp.amjpathol.org*, respectively. Genes expressed at relatively low levels in normal tissues and most of the nine non-C1 or -C2 tumors are designated by bar 2 in Figure 1 (for details see Supplemental Figure 3 at *http://ajp.amjpathol.org*). This group of genes includes multiple histone genes, *SON*, which encodes for a DNA-binding protein with sequence homology to *MYC* and *MOS* oncoproteins, and *CALU*, a gene that has been found to be down-regulated in metastatic head and neck squamous cell carcinoma relative to the primary tumor,[31] and associated with prognosis in MPM.[17] This provides evidence for the suggestion above that the non-C1 and -C2 tumors are inherently different from the other tumors at least with respect to the expression levels of certain genes. Furthermore, these gene expression patterns are likely responsible for the grouping of non-C1 or -C2 tumors nearer to normal tissues from unsupervised hierarchical cluster analysis. However, the high tumor cell content of these non-C1 and -C2 MPM samples is evident by examining the gene cluster desig-

Figure 2. Genes with elevated expression levels in C1 MPM tumors. Genes whose expression levels are elevated in C1 MPM tumors (from Figure 1) are shown in greater detail and annotated with gene symbol (ie, LocusLink identifier) and gene name (ie, Unigene title). Individual sample identifiers have been removed for the sake of clarity. Relative gene expression levels are given by the scale at the **bottom left**.

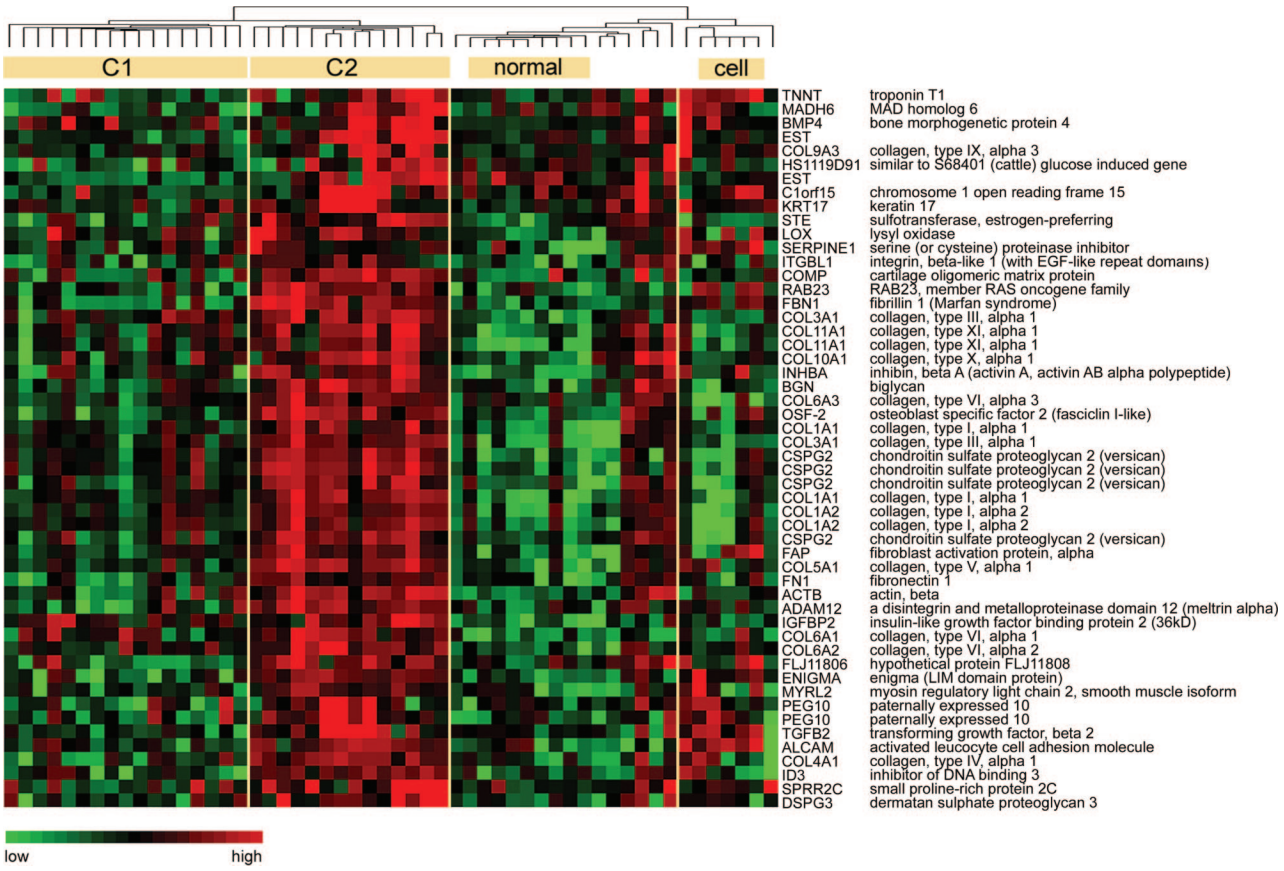

Figure 3. Genes with elevated expression levels in C2 MPM tumors. Genes whose expression levels are elevated in C2 MPM tumors (from Figure 1) are shown in greater detail and annotated with gene symbol (ie, LocusLink identifier) and gene name (ie, Unigene title). Individual sample identifiers have been removed for the sake of clarity. Relative gene expression levels are given by the scale at the **bottom left**.

nated by bar 4 in Figure 1 (for details see Supplemental Figure 5 at *http://ajp.amjpathol.org*) in which genes, such as surfactants and hemoglobin, that are typically expressed at high levels in normal lung and pleura are expressed at much lower levels in the relevant tumor tissues.

Genes overexpressed in C1 (Figure 2) include those with known or inferred function such as proto-oncogenes (eg, *MAF*, *MET*), tumor suppressors (eg, *GAS1*, *WT1*), and multiple genes associated with cytoskeletal/support (eg, keratins, cadherins, and other proteoglycans), signaling (eg, *KDR*), apoptosis (eg, *MST4*), and proliferation (eg, *FGF18*). A large number of C1-overexpressed genes have not been previously described in MPM and/or were initially characterized in other tissue types. For example, *NMU* codes for a neuropeptide with potent effects on smooth muscle contraction. Its role, if any, in MPM (or cancer in general) is unknown. Several C1-overexpressed genes are of particular interest. *CD47* is a gene that has been implicated in diverse cellular functions such as tumor cell chemotaxis,[32] integrin function,[33] and apoptosis.[34] The c-Met proto-oncogene (*MET*) has widely documented roles in tumorigenesis. Moreover, high levels of *MET* mRNA and protein have been previously found in MPM tumors and cell lines[35,36] and have been proposed to promote angiogenesis[37] and cell motility.[38] Recent evidence suggests that the *MET* pathway can be activated by SV40,[39] an interesting observation considering the unclear role of this virus in MPM etiology. Finally, we observed high mRNA levels of the *PLA2G2A* gene in C1 tumors. This gene is highly expressed in many other neoplasms where it has been proposed to promote carcinogenesis[40] or mediate profound anti-tumor effects[41] in a tissue/disease-specific manner. These latter observations are consistent with our previous studies showing *PLA2G2A* to be preferentially expressed in MPM tumors from patients with relatively good prognosis.[18]

Genes highly expressed in subclass C2 are listed in Figure 3 and consist mainly of extracellular matrix and structural proteins such as collagen, actin, biglycan, and fibronectin. Several of these genes (eg, *COMP*) are typically expressed in other tissue types and in less differentiated cells. This combined with an overall anabolic expression profile is consistent with the morphological appearance and clinical behavior of mixed histological subtype (ie, C2 subclass) MPM tumors. We also discovered at least two potentially interesting (nonmatrix-related) genes overexpressed in C2: *RAB23* and *BMP4*. RAB proteins are small GTPases that are members of the RAS superfamily and *RAB23* encodes a protein that is a negative regulator of the Sonic hedgehog signaling pathway.[42] This pathway is important in mammalian embryogenesis and its activation in adults can result in various tumors including a

subset of non-small cell lung cancers.[43] *BMP4* is another Sonic hedgehog pathway regulator that is also highly expressed in C2 tumors, and together these genes may indicate a potential role for this pathway in MPM. A complete listing of the 113 genes with average expression levels that were significantly different between C1 and C2 tumors is found in Supplemental Table 2 at *http://ajp.amjpathol.org*. Using SAM, we estimated a false-discovery rate of 15% for this gene list.

Identification of MPM Histological Molecular Markers

We identified those genes with expression patterns that were reflective of MPM histological subtype and found a total 54 genes with average expression levels significantly different between MPM histological classes with a false-discovery rate of ~15% (Supplemental Table 3 at *http://ajp.amjpathol.org*). Twenty-five and twenty-nine of these genes were expressed at relatively higher levels in epithelial and mixed MPM tumors, respectively. In fact, many of the genes that we found to be distinctive of C1 and C2 subclasses from hierarchical clustering were also differentially expressed in a statistically significant manner between epithelial and nonepithelial tumors. This finding provides additional evidence that the morphological appearance of MPM tumor cells may reflect distinct gene expression patterns.

Identification of MPM Tumor Molecular Markers

In a related analysis, we identified 328 genes that were differentially expressed at significantly higher levels in MPM tumors and 311 genes that were differentially expressed at significantly higher levels in all normal samples with an estimated false-discovery rate of 10% for both gene lists (Supplemental Table 4 at *http://ajp.amjpathol.org*). Among those genes significantly underexpressed in MPM tumor tissues was gelsolin (*GSN*, $P = 7.4 \times 10^{-8}$), a gene known to be down-regulated in multiple neoplasms and capable of suppressing tumorigenicity by inhibiting protein kinase C activation.[44] In this study, elevated *GSN* levels in the lung cancer cell line PC10 resulted in decreased proliferation *in vitro* and complete inhibition of tumorigenicity in *nude* mice.

By visually scanning the list of genes up-regulated in MPM, we noticed several genes that had known physiological roles suggestive of a role in carcinogenesis including platelet-derived growth factor C (*PDGFC*, $P = 0.018$) CREBBP/EP300 inhibitory protein 1 (*CRI1*, $P = 2.7 \times 10^{-4}$), and nucleoside-diphosphate kinase 2 (*NME2*, $P = 1.5 \times 10^{-9}$). These genes have well documented roles in growth and/or differentiation in multiple cancers, but have not previously been implicated in MPM pathogenesis.

Platelet-derived growth factor (PDGF) family members have been previously described in MPM,[8] and PDGF-C has been recently described as a novel transforming growth factor[45] that participates in an autocrine signaling loop.[46] Blocking of the functional receptor reduces tumor formation in *nude* mice.[46] The PDGF receptor is a tyrosine kinase that functions in the Akt and MAPK pathways, but is not likely involved with Erk phosphorylation.[46] PDGF-C has a binding pattern similar to PDGF (A and B) and, of particular note for MPM, is a more potent mitogen than either in cells of mesenchymal origin.[47] PDGF-C is highly expressed specifically in mesenchymal precursors and the myoblasts of smooth and skeletal muscle.[48]

The *NME2* gene is a transcriptional regulator with diverse functions that binds and cleaves DNA via covalent bond formation and catalyzes phosphoryl transfer.[49] It is a transcriptional regulator of specific genes (eg, activation of c-*MYC*) in a cell- and tissue-specific manner, is part of the N-*MYC* downstream pathway, and experimental evidence suggests that high levels of *NME2* are mutagenic.[50] NME2 protein has also been implicated in signal transduction pathways[51] and in control of cell adhesion and migration.[52] Finally, NME2 protein has been shown to bind single-stranded telomeric DNA and the RNA component of telomerase.[53] The physiological role of this interaction (if any) has yet to be determined. Recently, however, NME2 immunoreactivity was shown to be positively associated in a statistically significant manner with telomerase activity in hepatocellular carcinoma.[54]

CRI1 (also known as EID-1) is a CREB-binding protein and potential oncogene that, in functional assays, antagonizes the action of pRb, p300, and CREB-binding protein (CBP) histone acetylase activity.[55,56] Although CRI1 is capable of binding and sequestering wild-type unphosphorylated (active) pRb, there is also evidence that CRI1 acts at points downstream of pRb in differentiation and proliferation control pathways.[55] These observations are particularly notable in the context of mesothelioma because, although mutational or deletional loss of pRb is rare in most tumor types including MPM,[11] many MPMs are found to have deletions, mutations, or promoter methylation of $p16^{INK4a}$,[57] a regulator of pRb via inhibitory action on cdk4.

Validation of Microarray Data

To initially validate microarray data, we performed quantitative RT-PCR for *NME2* and *GSN* in all samples profiled with microarrays. (To facilitate comparison between platforms, we stated the expression level of both experimental genes relative to those of *GAPDH* in each sample.) We compared gene expression levels generated from quantitative RT-PCR to those from microarray analysis and found that the relative ranking of all tissues was relatively similar in both data acquisition platforms. For example, of the 10 MPM tumors with the highest and lowest *NME2* levels from microarray analysis, a total of 8 and 7 were similarly ranked, respectively, using quantitative RT-PCR. Similar results were obtained for *GSN*.

To determine whether these genes are useful for study *in vitro* and additionally validate microarray data, we quantified the mRNA levels of all three genes up-regulated in MPM (*PDGFC*, *CRI1*, *NME2*) in four MPM cell lines and HM3 cells, a normal (nontransformed) mesothelial

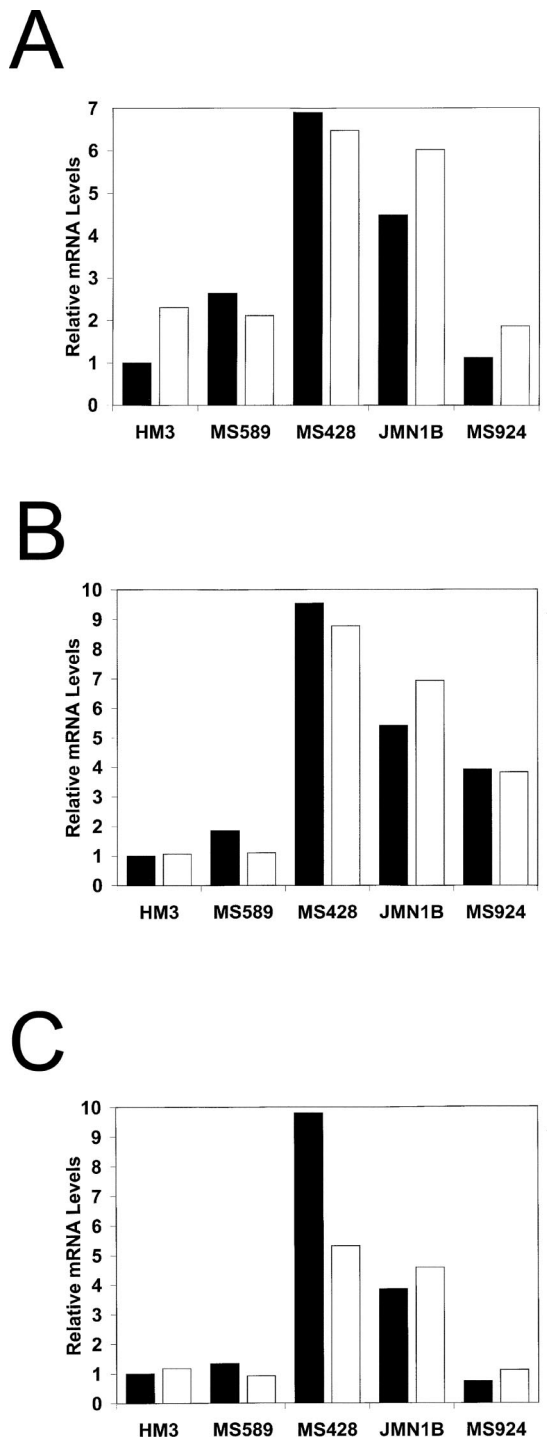

Figure 4. Validation of select MPM molecular markers. We examined, in normal and tumor cell lines with and without EGF in the culture medium, the mRNA levels of three genes that were found to be significantly differentially expressed between MPM tumors and normal tissues, as described in the text. We performed quantitative RT-PCR using four MPM cell lines (MS589, MS428, MS924, and JMN1B) and one normal mesothelial cell line (HM3). Individual mRNA levels were normalized to GAPDH and expressed relative to those in HM3 cells (−EGF) for *CRI1* (**A**), *NME2* (**B**), and *PDGFC* (**C**). Expression levels for tumor markers were typically at least twofold higher in tumor cell lines relative to HM3 (−EGF) cells for all three genes. **Black bars**, −EGF; **white bars**, +EGF.

cell line[58] not profiled using microarrays, with and without EGF in the culture medium as a control for the proliferation status of the cells (Figure 4). Both conditions (ie, ±EGF) permitted the growth of the MPM lines, but the −EGF condition induced a growth-arrested state for HM3 cells, as described previously.[28] We found that expression levels were typically higher in tumor cell lines relative to growth-arrested (−EGF) HM3 cells. EGF produced a twofold increase in *CRI1* mRNA levels for HM3 cells, but no or little increase for the tumor lines, suggesting that the MPM cell lines were no longer dependent on exogenous mitogen for expression of this gene (Figure 4A). Curiously, one tumor cell line (MS428) exhibited a twofold decrease in *PDGFC* mRNA in the presence of EGF (Figure 4C).

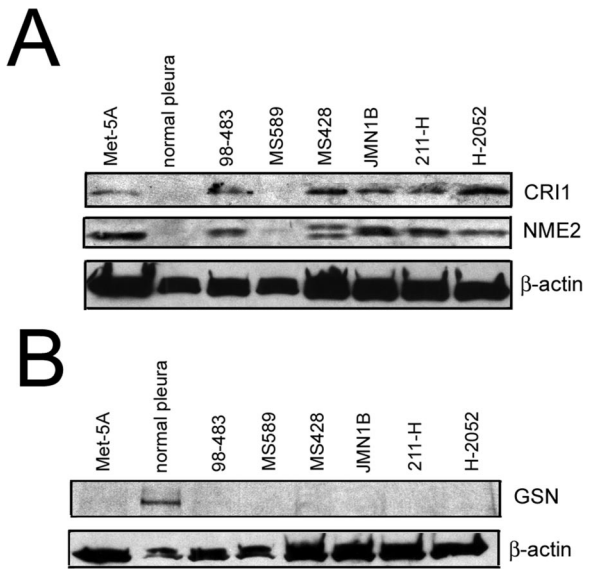

Figure 5. Protein analysis of candidate MPM tumor-related genes *in vitro*. Western blot analysis was performed for CRI1 and NME2 (**A**) and GSN (**B**) in nontumorigenic SV40-immortalized mesothelial cells (Met-5A) and six human MPM cell lines (98-483, MS589, MS428, JMN1B, 211-H, H-2052) as described in the Materials and Methods using β-actin as a loading control and pooled normal pleura as a control tissue.

Validation of a Previously Described MPM Diagnostic Test

MPM can be difficult to distinguish from lung adenocarcinoma without a surgical biopsy in patients presenting with unilateral malignant pleural effusion. We have previously described a simple, but highly accurate test based on the ratios of the expression levels of six genes that can overcome this difficulty. This test uses the combined score (ie, geometric mean; see Materials and Methods) of three gene pair ratios to distinguish between lung adenocarcinoma and MPM: calretinin/claudin-7, VAC-β/TACSTD1, MRC-OX/TITF.[13] Using quantitative RT-PCR, we obtained the relative expression level of each of these six genes in the 40 MPM tumors profiled in the current study and used these data to calculate the combined score of the three diagnostic ratios. As per the original publication,[13] samples with a combined score >1 and <1 were called MPM and lung adenocarcinoma, respectively. We found that this test was 97.5% accurate with a single MPM tumor being misdiagnosed (tumor 36).

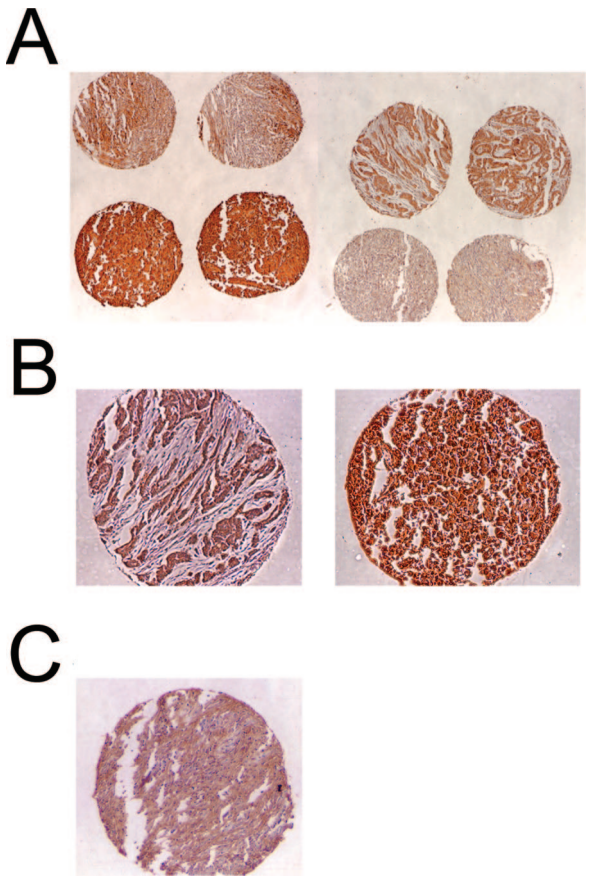

Figure 6. Protein analysis of candidate MPM tumor-related genes in human MPM tissues. We performed indirect immunohistochemical analysis of MPM tissue arrays consisting of 66 MPM tumors, 2 lung adenocarcinoma tumors, and 4 normal pleura tissues using antibodies to NME2 (**A** and **B**) and CRI1 (**C**). Expression of NME2 antigen varied widely in intensity in a diverse percentage of tumor cells (see Table 1), while CRI1 antigen was consistently expressed at moderate levels in all tumors examined. Neither protein was detected in normal pleura tissue or stromal elements of tumor tissues. Original magnifications: ×4 (**A**); ×10 (**B** and **C**).

Protein Analysis of MPM Candidate Oncogenes and Tumor Suppressors

A subset of MPM candidate oncogenes and tumor suppressors from above were examined for protein expression in MPM cell lines using Western blot analysis (Figure 5) and in MPM tumors using immunohistochemical analysis of an MPM tissue array (Figure 6). CRI1 protein was detected in four of the five MPM cell lines examined but not in normal pleural tissue (Figure 5A). No CRI1 protein was detected in MS589 cells, consistent with mRNA levels from Figure 4A. CRI1 was also faintly detected in the Met-5A cell line. Protein levels of NME2 had approximately similar expression patterns in Met-5A, MPM cell lines, and normal pleura (Figure 5A). Two bands of similar molecular weight were recognized by the anti-NME2 antibody in MS428 cell lysates. The cause of this phenomenon is unknown and occurs in a small number of cell lines (eg, HeLa and K562 cells; personal communication, Santa Cruz Biotechnology). GSN protein was only detected in normal pleural tissue and not in any cell line examined (Figure 5B). These results provide evidence that transcription and translation are coupled for *NME2* and *CRI1* (compare Figures 4 and 5). Of note, CRI1 and NME2 were both detected in the Met-5A cell line. One explanation for this observation is that MPM cells acquire expression of these (and other) candidate oncogenes in a stepwise progression during tumorigenesis because Met-5A, while nontumorigenic, is a mesothelial cell-derived SV40-immortalized cell line.

Table 1. Scoring of NME2 Protein Expression in MPM Tissue Array

Positive cells	Tissue type				
	Ept	Mixed	Sarc	ADCA	Np
0	10	5	1	1	4
<25%	10	6	1	1	
25–50%	5	1			
50–75%	7	5			
>75%	13	2			

Column/row intersections represent the distribution of normal and tumor tissues with NME2 protein expression detected in an increasing number of cells. For tumor tissues, only tumor cells were used for quantification and not surrounding stromal cells, which were consistently negative for NME2 protein.

Ept, MPM epithelial subtype; mixed, MPM mixed subtype; Sarc, MPM sarcomatoid subtype; ADCA, lung adenocarcinoma; Np, normal pleura.

NME2 protein showed variable and heterogeneous expression in the normal and tumor tissues present on the MPM tissue array (Figure 6, A and B, and Table 1). It is important to note that no NME2 protein was detected in any normal pleura tissue or in stromal cells from tumor tissues. NME2 protein was detected in a small number of tumor cells in both lung adenocarcinoma tissues and the MPM sarcomatoid histological subtype. The majority of epithelial (78%, 35 of 45) and mixed (74%, 14 of 19) MPM subtypes had detectable NME2 protein. Nearly half of all epithelial (44%, 20 of 45) and one-third of mixed (37%, 7 of 19) MPM subtypes had NME2 expression in at least 50% of tumor cells. When NME2 protein was detected, it was nearly always present at high levels with 74% (26 of 35) and 86% (12 of 14) of epithelial and mixed subtypes scored as strong expression, respectively. There was no statistically significant correlation between histological subtype and NME2 protein expression with respect to positive and negative cases, strongly and weakly staining cases, or to cases with moderate and extensive staining (ie, <50% and >50% of tumor cells positive, respectively). CRI1 protein expression displayed a more homogenous staining pattern on the MPM tissue array (see representative MPM tissue in Figure 6C). Similar to NME2 expression, CRI1 protein was not detected in any of the normal pleura tissues or stromal elements in tumor tissues, but was detected in nearly all tumor cells from MPM and lung adenocarcinoma tissues.

Pathway Analysis of MPM Candidate Oncogenes

We analyzed all 328 genes found to be statistically significantly up-regulated in MPM tumors relative to normal tissues from above to discover novel pathophysiological

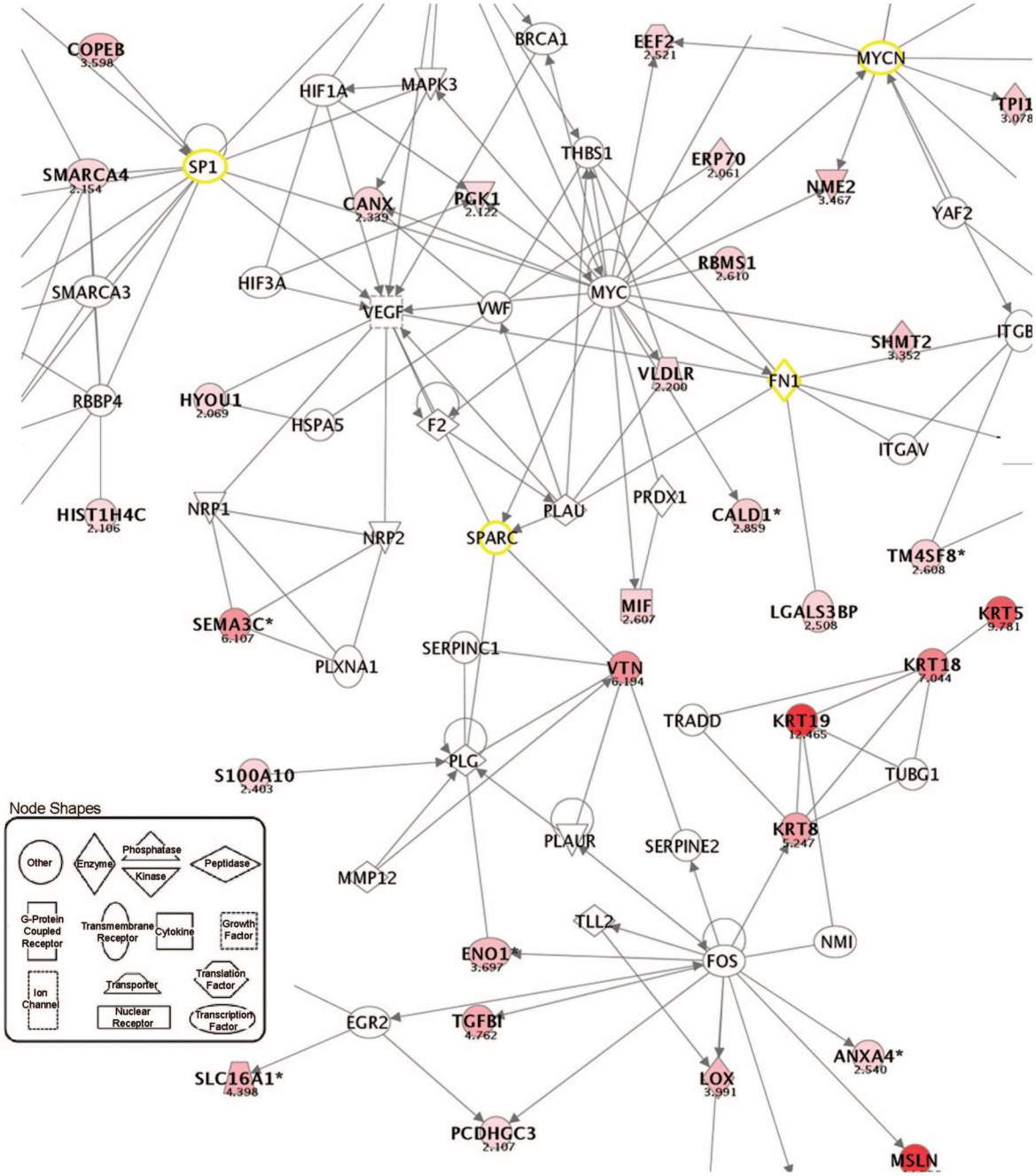

Figure 7. Pathway analysis of candidate MPM tumor-related genes. Genes found to be statistically significantly up-regulated in MPM were used to create a combined network of physiological pathways as described in the Materials and Methods. A portion of the resulting pathway is shown here. The intensity of the node color (red) indicates the experimentally determined degree of up-regulation of MPM tumor-associated genes expressed as a fold-increase in average expression levels relative to normal tissues. Other node colors are white (genes that are not user specified but are incorporated in networks through relationships with other genes) and yellow (genes that are shared by two or more networks in a merged diagram). Nodes are displayed using various shapes that represent the functional class of the gene product (see legend). Edges are displayed with various labels and shapes that describe the nature of the relationship between the nodes (eg, B for binding, T for transcriptional regulation) and links to experimental results and gene summaries supporting such a relationship. The edge labels and shapes have been removed from the diagram for the sake of clarity but can be found in Supplemental Figure 7 at *http://ajp.amjpathol.org*. The length of an edge reflects the evidence supporting that node-to-node relationship. Edges supported by more articles from the literature are shorter. For simplicity, genes are referred to by their LocusLink symbol.

pathways with potential relevance to MPM. Genes that were unknown (ie, expressed sequence tags) or uncharacterized in the scientific literature were discarded. We discovered a total of 12 networks, 7 of which had at least one gene in common and were merged for display. An enlarged portion of the resulting network is shown in Figure 7 and a high-resolution picture of the entire network can be found in Supplemental Figure 7 at *http://ajp.amjpathol.org*. The combined network consisted of 210 genes, approximately half of which (46%, 97 of 210) were MPM up-regulated genes. (For simplicity, genes are referred to by their LocusLink symbol in Figure 7 and the

text.) Five genes (*TP53*, *SP1*, *SPARC*, *FN1*, *MYCN*) were shared by at least two networks. Of these, *SP1* and *SPARC* were not previously described in MPM in the published scientific literature. The *SP1* transcription factor has multiple functions and can drive the expression of many cancer-related genes such as *VEGF*. SPARC (also known as osteonectin, *ON*) is a matrix-associated protein that can elicit changes in cell shape, inhibit cell-cycle progression, and influence the synthesis of extracellular matrix. Note in Figure 7 that SPARC binds to and modulates vitronectin (VTN), an MPM up-regulated gene that promotes cell adhesion and spreading. Pathway analysis revealed that the SPARC/VTN interaction can also modulate adhesion and spreading of endothelial cells, which may function in angiogenesis in the context of MPM tumorigenesis.

We found it interesting that several *MYCN*-regulated genes are highly expressed in MPM tumors (including *NME2* which is also regulated by *MYC*) even though *MYCN* is not generally thought to play a role in MPM carcinogenesis (Figure 7). Although MPM tumors and cell lines contained low, but reliably detectable levels of *MYCN* mRNA by microarray analysis, this gene may be physiologically relevant during MPM tumorigenesis because MYCN protein has been detected in some MPM tumors,[59] and not all neuroblastoma tumors or cell lines have *MYCN* genomic amplification yet still contain detectable mRNA and protein.[60] Alternatively, genes regulated by multiple *myc* family members could be transcriptionally activated primarily by *MYC* in MPM.

Other genes forming prominent nodes in pathway analysis include well-studied transcription factors regulating proliferation and apoptosis (*E2F1*, *E2F4*, *FOS*, *MYC*), cell cycle regulators (*RB1*), and growth factors (*VEGF*). Several of these networks contain genes that have been previously described in MPM and/or are consistent with current knowledge. For example, the up-regulation of genes transcriptionally regulated by *TP53* and *RB1* tumor suppressors is consistent with the lack of mutations in these genes in MPM.[9–11] Similarly, *VEGF* and *MYC* have been previously described as potential proto-oncogenes in MPM.[8] Curiously, we found high levels of the *FMR1* gene in MPM tumors. Mutations in this gene are responsible for X-linked mental retardation (ie, fragile X syndrome) and the role of this gene (if any) in cancer is unknown. This mRNA binding protein has not previously been described in MPM and forms a node with other genes that have mRNA to which it is capable of binding. These genes (eg, *GNAS*, *SPP1*, *CDK4*, *HINT1*, *COLL11A1*, *CDH11*, *CBX3*) are themselves up-regulated in MPM. Although the exact functional relevance of these results is unknown at present, at least one of these genes is in a pathway with direct cancer relevance (eg, *SPP1*, which interacts with the anti-apoptotic protein IGFBP2, also expressed at high mRNA levels in MPM).

In other studies, investigators have found that AP-1 transcription factor family members *FOS* and *FOSL1* (also known as *fra-1*) were associated with MPM tumorigenesis, consistent with our pathway analysis showing that multiple MPM up-regulated gene products form a node with *FOS* (Figure 7). In these analyses, *FOSL1* mRNA levels were found to be elevated in both rat mesothelioma cell lines and rat mesothelial cells exposed to asbestos, but *FOS* mRNA levels were up-regulated only in the latter.[61–64] This finding prompted these investigators to suggest that *FOSL1* may substitute for *FOS* in AP-1 complexes during human MPM tumorigenesis.[62] Consistent with these findings, we have also observed relatively low (or absent) mRNA levels of *FOS* and substantially higher mRNA levels of *FOSL1* in human MPM cell lines in the current study and in those cell lines previously profiled with microarrays in our laboratory.[13] However, we observed *FOS* mRNA levels that are 56-fold higher than those of *FOSL1* in the human MPM specimens profiled in the current study, consistent with a similar eightfold difference previously observed.[13] In fact, the average expression level of *FOS* in human MPM tumors in the current study is in the 98th percentile relative to the average expression level of all of the genes represented on the microarray. The high intertumor variability of *FOS* expression levels (average, 1009; range, 5.7 to 3718) accounts for the fact that it is not statistically significantly elevated compared to normal tissues. Despite the lack of *FOS* mRNA in rat and human MPM cell lines in our studies and others, the high levels of this gene in human MPM tumors necessitates its continued study in MPM pathogenesis.

Several of the genes highly expressed in MPM relative to normal tissues have been previously shown to have prognostic value in MPM. Pass and colleagues[17] profiled 21 MPM patients and created a 27-gene neural network classifier that could predict clinical outcome with high accuracy. Of these 27 genes, 5 were found to be statistically significantly up-regulated in MPM in the current study (*CRIP1*, *IGFBP5*, *KIAA0275*, *KIAA1237*, *MYC*). It is noteworthy that *NME1* was reported as a prognostic gene in MPM by these authors.[17] This gene is highly related to *NME2*, a tumor marker discovered in the current study. Clearly, this family of genes is important in MPM and deserves additional study.

In this report we describe an extensive transcriptional analysis of MPM tumors leading to the identification of at least two possible subclasses of MPM with different gene expression patterns that correlate loosely with tumor histology. We also identify and validate a subset of MPM tumor-related genes with aberrant expression that may contribute to MPM tumorigenesis. Finally, we performed pathway analysis of MPM candidate oncogenes to identify potential cellular pathways, the dysregulation of which may contribute to and/or reflect MPM tumorigenesis and pathogenesis.

References

1. Britton M: The epidemiology of mesothelioma. Semin Surg Oncol 2002, 29:18–25
2. Pass H: Malignant pleural mesothelioma: surgical roles and novel therapies. Clin Lung Cancer 2001, 3:102–117
3. Peto J, Decarli A, La Vecchia C, Levi F, Negri E: The European mesothelioma epidemic. Br J Cancer 1999, 79:666–672
4. Peto J, Hodgson JT, Matthews FE, Jones JR: Continuing increase in mesothelioma mortality in Britain. Lancet 1995, 345:535–539
5. Sugarbaker DJ, Liptay MJ: Therapeutic approaches in malignant

mesothelioma. Comprehensive Textbook of Thoracic Oncology. Edited by Aisner J, Arriagada R, Green MR, Martini N, Perry MC. Baltimore, Williams and Wilkins, 1996, pp 786–798
6. Corson JM, Renshaw AA: Pathology of mesothelioma. Comprehensive Textbook of Thoracic Oncology. Edited by Aisner J, Arriagada R, Green MR, Martini N, Perry MC. Baltimore, Williams and Wilkins, 1996, pp 757–758
7. Sugarbaker DJ, Garcia JP, Richards WG, Harpole Jr DH, Healy-Baldini E, DeCamp Jr MM, Mentzer SJ, Liptay MJ, Strauss GM, Swanson SJ: Extrapleural pneumonectomy in the multimodality therapy of malignant pleural mesothelioma. Results in 120 consecutive patients. Ann Surg 1996, 224:288–294
8. Lechner JF, Tesfaigzi J, Gerwin BI: Oncogenes and tumor-suppressor genes in mesothelioma—a synopsis. Environ Health Perspect 1997, 105:1061–1067
9. Metcalf RA, Welsh JA, Bennet WP, Seddon MB, Lehman TA, Pelin K, Linnainmaa K, Tammilehto L, Mattson K, Gerwin BI, Harris CC: p53 and Kirsten-ras mutations in human mesothelioma cell lines. Cancer Res 1992, 52:2610–2615
10. Mor O, Yaron P, Huszar M, Yellin A, Kakobovitz O, Brok-Simoni F, Rechavi G, Reichart N: Absence of p53 mutations in malignant mesotheliomas. Am J Respir Cell Mol Biol 1997, 16:9–13
11. Van der Meeren A, Seddon MB, Kispert J, Harris CC, Gerwin BI: Lack of expression of the retinoblastoma gene is not frequently involved in the genesis of human mesothelioma. Eur Respir Rev 1993, 3:177–179
12. Carbone M, Rizzo P, Grimley PM, Procopio A, Mew DJY, Shridhar V, De Bartolomeis A, Esposito V, Giuliano MT, Steinberg SM, Levine AS, Giordano A, Pass HI: Simian virus-40 large-T antigen binds p53 in human mesothelioma. Nat Med 1997, 3:908–912
13. Gordon GJ, Jensen RV, Hsiao L-L, Gullans SR, Blumenstock JE, Ramaswami S, Richards WG, Sugarbaker DJ, Bueno R: Translation of microarray data into clinically relevant cancer diagnostic tests using gene expression ratios in lung cancer and mesothelioma. Cancer Res 2002, 62:4963–4967
14. Kettunen E, Nissen AM, Ollikainen T, Taavitsainen M, Tapper J, Mattson K, Linnainmaa K, Knuutila S, El-Rifai W: Gene expression profiling of malignant mesothelioma cell lines: cDNA array study. Int J Cancer 2001, 91:492–496
15. Rihn BH, Mohr S, McDowell SA, Binet S, Loubinoux J, Galateau F, Keith G, Leikauf GD: Differential gene expression in mesothelioma. FEBS Lett 2000, 480:95–100
16. Singhal S, Wiewrodt R, Malden LD, Amin KM, Matzie K, Friedberg J, Kucharczuk JC, Litzky LA, Johnson SW, Kaiser LR, Albelda SM: Gene expression profiling of malignant mesothelioma. Clin Cancer Res 2003, 9:3080–3097
17. Pass HI, Liu Z, Wali A, Bueno R, Land S, Lott D, Siddiq F, Lonardo F, Carbone M, Draghici S: Gene expression profiles predict survival and progression of pleural mesothelioma. Clin Cancer Res 2004, 10:849–859
18. Gordon GJ, Hsiao L-L, Jensen RV, Gullans SR, Blumenstock JE, Richards WG, Sugarbaker DJ, Bueno R: Using gene expression ratios to predict outcome among patients with mesothelioma. J Natl Cancer Inst 2003, 95:598–6058
19. Behbehani AM, Hunter WJ, Chapman AL, Lin F: Studies of a human mesothelioma. Hum Pathol 1982, 13:862–866
20. Demetri GD, Zenzie BW, Rheinwald JG, Griffin JD: Expression of colony-stimulating factor genes by normal human mesothelial cells and human malignant mesothelioma cells lines in vitro. Blood 1989, 74:940–946
21. Ke Y, Reddel RR, Gerwin BI, Reddel HK, Somers AN, McMenamin MG, LaVeck MA, Stahel RA, Lechner JF, Harris CC: Establishment of a human in vitro mesothelial cell model system for investigating mechanisms of asbestos-induced mesothelioma. Am J Pathol 1989, 134:979–991
22. Bepler G, Koehler A, Kiefer P, Havemann K, Beisenherz K, Jaques G, Gropp C, Haeder M: Characterization of the state of differentiation of six newly established human non-small-cell lung cancer cell lines. Differentiation 1988, 37:158–171
23. Quackenbush J: Computational analysis of microarray data. Nat Rev Genet 2001, 2:418–427
24. Eisen MB, Spellman PT, Brown PO, Botstein D: Cluster analysis and display of genome-wide expression patterns. Proc Natl Acad Sci USA 1998, 95:14863–14868
25. Kaufman L, Rousseeuw PJ: Finding Groups in Data: An Introduction to Cluster Analysis. New York, Wiley, 1990
26. Venables WN, Riley BD: Modern Applied Statistics with S-Plus. New York, Springer, 1997
27. Tusher VG, Tibshirani R, Chu G: Significance analysis of microarrays applied to the ionizing radiation response. Proc Natl Acad Sci USA 2001, 98:5116–5121
28. Connell ND, Rheinwald JG: Regulation of the cytoskeleton in mesothelial cells: reversible loss of keratin and increase in vimentin during rapid growth in culture. Cell 1983, 34:245–253
29. Rheinwald JG, Hahn WC, Ramsey MR, Wu JY, Guo ZS, Tsao H, De Luca M, Catricala C, O'Toole KM: A two-stage, p16(INK4A)- and p53-dependent keratinocyte senescence mechanism that limits replicative potential independent of telomere status. Mol Cell Biol 2002, 22:5157–5172
30. Gordon GJ, Chen C-J, Mukhopadhyay NK, Jaklitsch MWG, Sugarbaker DJ, Bueno R: Inhibitor of apoptosis protein-1 promotes tumor cell survival in mesothelioma. Carcinogenesis 2002, 23:1017–1024
31. Wu W, Tang X, Hu W, Lotan R, Hong WK, Mao L: Identification and validation of metastasis-associated proteins in head and neck cancer cell lines by two-dimensional electrophoresis and mass spectrometry. Clin Exp Metastasis 2002, 19:319–326
32. Shahan TA, Fawzi A, Bellon G, Monboisse JC, Kefalides NA: Regulation of tumor cell chemotaxis by type IV collagen is mediated by a Ca(2+)-dependent mechanism requiring CD47 and the integrin alpha(V)beta(3). J Biol Chem 2000, 275:4796–4802
33. Barazi HO, Li Z, Cashel JA, Krutzsch HC, Annis DS, Mosher DF, Roberts DD: Regulation of integrin function by CD47 ligands. Differential effects on alpha vbeta 3 and alpha 4beta1 integrin-mediated adhesion. J Biol Chem 2002, 277:42859–42866
34. Mateo V, Lagneaux L, Bron D, Biron G, Armant M, Delespesse G, Sarfati M: CD47 ligation induces caspase-independent cell death in chronic lymphocytic leukemia. Nat Med 1999, 5:1277–1284
35. Harvey P, Warn A, Newman P, Perry LJ, Ball RY, Warn RM: Immunoreactivity for hepatocyte growth factor/scatter factor and its receptor, met, in human lung carcinomas and malignant mesotheliomas. J Pathol 1996, 180:389–394
36. Thirkettle I, Harvey P, Hasleton PS, Ball RY, Warn RM: Immunoreactivity for cadherins, HGF/SF, met, and erbB-2 in pleural malignant mesotheliomas. Histopathology 2000, 36:522–528
37. Tolnay E, Kuhnen C, Wiethege T, Konig JE, Voss B, Muller KM: Hepatocyte growth factor/scatter factor and its receptor c-Met are overexpressed and associated with an increased microvessel density in malignant pleural mesothelioma. J Cancer Res Clin Oncol 1998, 124:291–296
38. Klominek J, Baskin B, Liu Z, Hauzenberger D: Hepatocyte growth factor/scatter factor stimulates chemotaxis and growth of malignant mesothelioma cells through c-met receptor. Int J Cancer 1998, 76:240–249
39. Cacciotti P, Libener R, Betta P, Martini F, Porta C, Procopio A, Strizzi L, Penengo L, Tognon M, Mutti L, Gaudino G: SV40 replication in human mesothelial cells induces HGF/Met receptor activation: a model for viral-related carcinogenesis of human malignant mesothelioma. Proc Natl Acad Sci USA 2001, 98:12032–12037
40. Longo WE, Grossmann EM, Erickson B, Panesar N, Mazuski JE, Kaminski DL: The effect of phospholipase A_2 inhibitors on proliferation and apoptosis of murine intestinal cells. J Surg Res 1999, 84:51–56
41. Cormier RT, Hong KH, Halberg RB, Hawkins TL, Richardson P, Mulherkar R, Dove WF, Lander ES: Secretory phospholipase Pla2g2a confers resistance to intestinal tumorigenesis. Nat Genet 1997, 17:88–91
42. Eggenschwiler JT, Espinoza E, Anderson KV: Rab23 is an essential negative regulator of the mouse Sonic hedgehog signalling pathway. Nature 2001, 412:194–198
43. Watkins DN, Berman DM, Burkholder SG, Wang B, Beachy PA, Baylin SB: Hedgehog signalling within airway epithelial progenitors and in small-cell lung cancer. Nature 2003, 422:313–317
44. Sagawa N, Fujita H, Banno Y, Nozawa Y, Katoh H, Kuzumaki N: Gelsolin suppresses tumorigenicity through inhibiting PKC activation in a human lung cancer cell line, PC10. Br J Cancer 2003, 88:606–612
45. Zwerner JP, May WA: Dominant negative PDGF-C inhibits growth of Ewing family tumor cell lines. Oncogene 2002, 21:3847–3854

46. Lokker NA, Sullivan CM, Hollenbach SJ, Israel MA, Giese NA: Platelet-derived growth factor (PDGF) autocrine signaling regulates survival and mitogenic pathways in glioblastoma cells: evidence that the novel PDGF-C and PDGF-D ligands may play a role in the development of brain tumors. Cancer Res 2002, 62:3729–3735
47. Gilbertson DG, Duff ME, West JW, Kelly JD, Sheppard PO, Hofstrand PD, Gao Z, Shoemaker K, Bukowski TR, Moore M, Feldhaus AL, Humes JM, Palmer TE, Hart CE: Platelet-derived growth factor C (PDGF-C), a novel growth factor that binds to PDGF alpha and beta receptor. J Biol Chem 2001, 276:27406–27414
48. Ding H, Wu X, Kim I, Tam PP, Koh GY, Nagy A: The mouse Pdgfc gene: dynamic expression in embryonic tissues during organogenesis. Mech Dev 2000, 96:209–213
49. Postel EH, Abramczyk BA, Gursky SK, Xu Y: Structure-based mutational and functional analysis identify human NM23–H2 as a multifunctional enzyme. Biochemistry 2002, 41:6330–6337
50. Postel EH: Multiple biochemical activities of NM23/NDP kinase in gene regulation. J Bioenerg Biomembr 2003, 35:31–40
51. Kimura N, Shimada N, Ishijima Y, Fukuda M, Takagi Y, Ishikawa N: Nucleoside diphosphate kinases in mammalian signal transduction systems: recent developments and perspective. J Bioenerg Biomembr 2003, 35:41–47
52. Fournier H-N, Albigès-Rizo C, Block MR: New insights into Nm23 control of cell adhesion and migration. J Bioenerg Biomembr 2003, 35:81–87
53. Lombardi D, Mileo AM: Protein interactions provide new insight into Nm23/nucleoside diphosphate kinase functions. J Bioenerg Biomembr 2003, 35:67–71
54. Iizuka N, Mori N, Tamesa T, Tangoku A, Oka M: Telomerase activity and Nm23–H2 protein expression in hepatocellular carcinoma. Anticancer Res 2003, 23:43–47
55. Miyake S, Sellers WR, Safran M, Li X, Zhao W, Grossman SR, Gan J, DeCaprio JA, Adams PD, Kaelin Jr WG: Cells degrade a novel inhibitor of differentiation with E1A-like properties upon exiting the cell cycle. Mol Cell Biol 2000, 20:8889–8902
56. MacLellan WR, Xiao G, Abdellatif M, Schneider MD: A novel Rb- and p300-binding protein inhibits transactivation by MyoD. Mol Cell Biol 2000, 20:8903–8915
57. Hirao T, Bueno R, Chen CJ, Gordon GJ, Heilig E, Kelsey KT: Alterations of the p16(INK4) locus in human malignant mesothelial tumors. Carcinogenesis 2002, 23:1127–1130
58. Murphy JE, Rheinwald JG: Intraperitoneal injection of genetically modified, human mesothelial cells for systemic gene therapy. Hum Gene Ther 1997, 8:1867–1879
59. Kishimoto T: The distribution of various type of oncogenes products in the tumor tissue of malignant mesothelioma. Nihon Kyobu Shikkan Gakkai Zasshi 1991, 29:1168–1173
60. Tsuchida Y, Hemmi H, Inoue A, Obana K, Yang HW, Hayashi Y, Kanda N, Shimatake H: Genetic clinical markers of human neuroblastoma with special reference to N-myc oncogene: amplified or not amplified? Tumour Biol 1996, 17:65–74
61. Ramos-Nino ME, Timblin CR, Mossman BT: Mesothelial cell transformation requires increased AP-1 binding activity and ERK-dependent Fra-1 expression. Cancer Res 2002, 62:6065–6069
62. Ramos-Nino ME, Scapoli L, Matrtinelli M, Land S, Mossman BT: Microarray analysis and RNA silencing link fra-1 to cd44 and c-met expression in mesothelioma. Cancer Res 2003, 63:3539–3545
63. Heintz N, Janssen Y, Mossman BT: Persistent induction of c-fos and c-jun expression by asbestos. Proc Natl Acad Sci USA 1993, 90:3299–3303
64. Janssen Y, Heintz N, Marsh J, Borm P, Mossman BT: Induction of c-fos and c-jun protooncogenes in target cells of the lung and pleura by carcinogenic fibers. Am J Respir Cell Mol Biol 1994, 11:522–530